Nuclear Inst. and Methods in Physics Research, A 1033 (2022) 166640

Contents lists available at ScienceDirect

Nuclear Inst. and Methods in Physics Research, A

journal homepage: www.elsevier.com/locate/nima

DGFRS-2—A gas-filled recoil separator for the Dubna Super Heavy Element Factory

Yu.Ts. Oganessian [a], V.K. Utyonkov [a], A.G. Popeko [a,*], D.I. Solovyev [a], F.Sh. Abdullin [a], S.N. Dmitriev [a], D. Ibadullayev [a,b], M.G. Itkis [a], N.D. Kovrizhnykh [a], D.A. Kuznetsov [a], O.V. Petrushkin [a], A.V. Podshibiakin [a], A.N. Polyakov [a], R.N. Sagaidak [a], L. Schlattauer [a,c], I.V. Shirokovsky [a], V.D. Shubin [a], M.V. Shumeiko [a], Yu.S. Tsyganov [a], A.A. Voinov [a], V.G. Subbotin [a], V.V. Bekhterev [a], N.A. Belykh [a], O.A. Chernyshev [a], K.B. Gikal [a], G.N. Ivanov [a], A.V. Khalkin [a], V.V. Konstantinov [a], N.F. Osipov [a], S.V. Paschenko [a], A.A. Protasov [a], V.A. Semin [a], V.V. Sorokoumov [a], K.P. Sychev [a], V.A. Verevochkin [a], B.I. Yakovlev [a], S. Antoine [d], W. Beeckman [d], P. Jehanno [d], M.I. Yavor [e], A.P. Shcherbakov [e], K.P. Rykaczewski [f], T.T. King [f], J.B. Roberto [f], N.T. Brewer [f,1], R.K. Grzywacz [f,g], Z.G. Gan [h], Z.Y. Zhang [h], M.H. Huang [h], H.B. Yang [h]

[a] Joint Institute for Nuclear Research, 141980 Dubna, Russian Federation
[b] Institute of Nuclear Physics, 050032 Almaty, Kazakhstan
[c] Palacky University Olomouc, Department of Experimental Physics, Faculty of Science, 771 46 Olomouc, Czech Republic
[d] SIGMAPHI, F-56000 Vannes, France
[e] Institute for Analytical Instrumentation, RAS, 198103 St. Petersburg, Russian Federation
[f] Oak Ridge National Laboratory, Oak Ridge, TN 37831, USA
[g] Department of Physics and Astronomy, University of Tennessee, Knoxville, TN 37996, USA
[h] Institute of Modern Physics, Chinese Academy of Sciences, Lanzhou 730000, China

ARTICLE INFO

Keywords:
Electromagnetic separators
Gas-filled separators
Nuclear reactions
Superheavy elements

ABSTRACT

The main goal of development of the new **D**ubna **G**as-**F**illed **R**ecoil **S**eparator (DGFRS-2) is to sufficiently improve the efficiency of studies on heavy and superheavy nuclei at the Super Heavy Element Factory of the Flerov Laboratory of Nuclear Reactions (FLNR) at the Joint Institute for Nuclear Research. The use of beams with the intensity up to 6×10^{13} s^{-1} (10 pμA) delivered by the DC280 cyclotron requires an effective setup providing high suppression of background reaction products. The described gas-filled separator is optimized for synthesis and study of heavy isotopes produced in complete fusion reactions of massive nuclei. Basic characteristics of DGFRS-2, as well as the results of the first test experiments, are presented. In comparison to the DGFRS-1, the transmission efficiency was doubled, and the background was reduced by a factor 200.

1. Introduction

In experiments carried out over the past 20 years, the theory pointing to the existence of a region of superheavy elements (SHE) has received experimental confirmation. In complete-fusion reactions of ^{48}Ca with actinide (Act) targets the heaviest isotopes of Nh (Z = 113) and five new elements from Fl (Z = 114) to Og (Z = 118) were synthesized and the decay properties of more than 50 new heaviest isotopes of elements from Rf to Og have been studied [1,2]. The gas-filled separator DGFRS (further we will call it DGFRS-1), installed at the U400 cyclotron of FLNR in 1989 was used in these experiments. The principle of operation of a gas-filled separator has been often discussed in the literature, e.g. [3–6].

The synthesis of isotopes of heavier elements Z = 119 and Z = 120 using the heaviest available target materials ^{248}Cm, ^{249}Bk, ^{251}Cf requires the projectiles with higher atomic number Z like ^{50}Ti, ^{51}V, and ^{54}Cr. However, the cross-sections of fusion reactions with heavier projectiles are expected to be significantly lower than that with ^{48}Ca. In this regard, it is necessary to substantially increase the overall experiment efficiency.

* Corresponding author.
E-mail address: popeko@jinr.ru (A.G. Popeko).
[1] Current address: Premise Health, Brentwood, Tennessee 37027, USA.

https://doi.org/10.1016/j.nima.2022.166640
Received 20 January 2022; Received in revised form 22 March 2022; Accepted 31 March 2022
Available online 5 April 2022

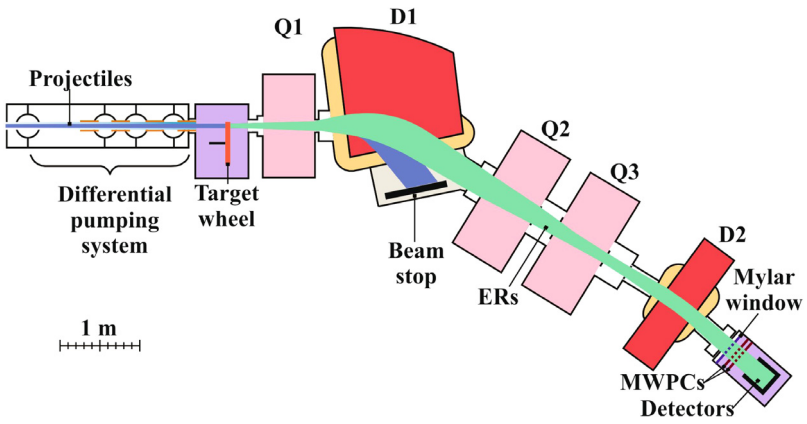

Fig. 1. Schematic layout of DGFRS-2.

Table 1
Data on known gas-filled online separators.

Set-up	Scheme	Bend. angle	$B{\cdot}\rho_{max}$ T m	Dispersion mm/% $B{\cdot}\rho$	Length m	Ref.
DGFRS-1	$D_vQ_hQ_v$	23°	3.1	7.5	4.07	[5]
BGS	Q_vD_hD	(25 + 45)°	2.5	20.0	4.6	[11]
GARIS-1	$D_{vh}Q_hQ_vD$	(45 + 10)°	2.16	9.7	5.76	[12]
TASCA	DQ_hQ_v	30°	2.4	9.0	3.5	[13]
GARIS-2	$Q_vD_hQ_hQ_vD$	(30 + 7)°	2.43	19.3	5.06	[14]
DGFRS-2	$Q_vD_hQ_hQ_vD$	(32 + 10)°	3.35	32.8	7.41	This work

To solve this problem and continue the research of superheavy nuclei, a new experimental facility — the Super Heavy Element Factory [7] was developed at FLNR. It includes the specialized high-current heavy ion cyclotron DC280 [8] capable producing beams of accelerated ions with an intensity 10 times higher than the existing U400 accelerator. The new gas-filled separator – DGFRS-2 with increased transmission of complete fusion reaction products – evaporation residues (ERs) and higher suppression factors of background particles is installed at one of the five beam lines of DC280.

The gas-filled separator DGFRS-1 was created in the late 80's [9] for experiments on the synthesis of superheavy elements. The studies performed at the initial stage revealed that in reactions leading to SHE the differences in magnetic rigidities of evaporation residues, target-like and projectile-like reaction products moving in hydrogen, are significantly larger than those of particles in helium [10]. Further experiments on the DGFRS-1 were carried out exclusively with the hydrogen filling, since better suppression of background is provided. However, it should be noted that this required ≈20% higher magnetic fields, both in deflecting magnets and in focusing lenses than in He. And there are additional safety concerns, since H_2 gas is flammable.

Table 1 shows the data on known gas-filled online separators used for the synthesis and study of superheavy nuclei. In the configuration description, D denotes a dipole magnet, D_v, D_h and D_{vh} are dipole magnets focusing in the vertical, horizontal or both directions, Q_h and Q_v mean horizontally and vertically focusing quadrupole lenses. Unlike DGFRS-1, all other separators are operated with helium filling.

2. Design of the DGFRS-2 separator

2.1. Design and simulations

When developing a separator, for the simulation of trajectories of particles passing through a magnetic system the Monte-Carlo computer code [15] has been used. The code generated "ERs" with the magnetic rigidity corresponding to the average ionic charge of particles moving in hydrogen. Using this code the factors leading to ER's losses when passing through DGFRS-1 were analyzed. It was found that the most significant reduction of transmitted recoils of ≈50% occurs when particles pass through the dipole magnet [16]. This is understandable, since it is difficult to find a compromise between a large aperture, high magnetic field strength, and the size and weight of the magnet. Thus it was proposed [17] to introduce a vertically focusing quadrupole lens in front of the dipole magnet, as it was done at BGS [11]. A second dipole magnet was introduced before the detector system to reduce the background from light particles.

For optimization of apertures, characteristics of magnetic elements and distances between them, the computer code [18] and the algorithms described in [19] have been used. In our case we have chosen the yield of ERs at the output of the system as the merit function which should be maximized. A series of calculations allowed one to obtain the optimal configuration of the new separator. The schematic layout of DGFRS-2 is shown in Fig. 1. It can be described in the form $Q_vD_hQ_hQ_vD$ (see Table 1).

The evaluation of the separator transmission and particle distribution on the focal plane requires taking into account the ion charge exchange during the passage through a gas filled magnetic system. One must remember that the ionic charge is an integer number. It means, that e.g. if the average charge $\bar{q} = 5.5$, the real charge can vary mostly between 4–5 and 6–7, and the deviation of the actual and average magnetic rigidity can be more than ±30%. This effect broadens both the horizontal and vertical distributions of particles.

To describe this process, data on charge-exchange cross-sections σ_{cc} of electron capture and loss would be necessary. Because such experimental data are scarce, we use for the simulation the N. Bohr's suggestion [20] about the relationship between the recharge exchanging processes with the scattering and energy loss of ions. The charge changing cross section was assumed to be $\sigma_{cc} \sim \pi a_{scr}^2$, where a_{scr} is the characteristic length of electronic screening of the bare nuclear charges Z_1 of the moving ion and Z_2 of gas. The randomly distributed flight pass l_{random} between collisions is evaluated using the relation $l_{random} \sim (-\ln(1-R))/(\sigma_{cc} * N_H * P)$, where R is a random number between 0 and 1 (0 included, 1 excluded), $N_H = 5.303 \cdot 10^{16}$ is a number of

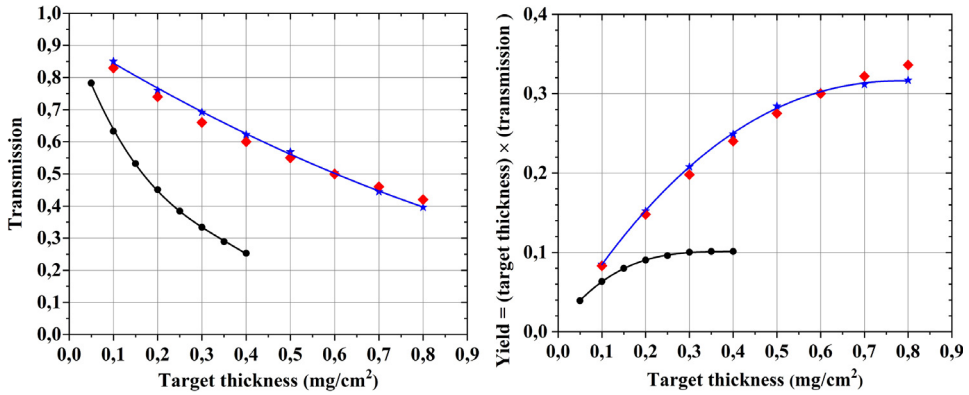

Fig. 2. Results of ion-optical calculations and simulations of transmission (left panel) and yield (right panel) of ^{288}Fl produced in the ^{244}Pu(^{48}Ca,4n)^{288}Fl reaction for DGFRS-2 (upper blue lines with stars) and DGFRS-1 (lower black lines and symbols) as a function of the PuO_2 target thickness. Red diamonds show the results of modeling described in Section 3 for the same reaction.

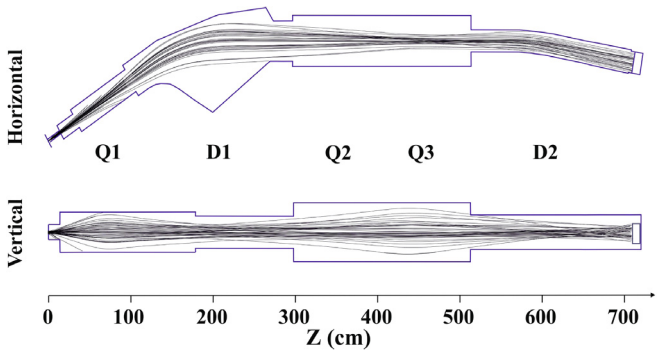

Fig. 3. Trajectories of ERs simulated using GEANT4 platform.

hydrogen atoms in cm^3 at 1 mbar pressure, P is a gas pressure in mbar. At each point of interaction the random integer charge state will be generated according to a normal or chi-squared — χ^2 [21] distributions with $\bar{q}$ and a standard charge deviation determined according to [22].

The results of Monte Carlo simulations of transmission and yield of ^{288}Fl produced in the ^{244}Pu(^{48}Ca,4n)^{288}Fl reaction for DGFRS-2 and DGFRS-1 as a function of the PuO_2 target thickness are compared in Fig. 2. The calculations considered a Gaussian shaped excitation function having for ^{48}Ca + Act fusion reactions FWHM ≈ 10 MeV [23]. The analysis showed that the overall efficiency of DGFRS-2 was expected to be higher by a factor of 2.0–2.5 in comparison to that of DGFRS-1 for typical targets of 0.3–0.4 mg/cm^2. The momentum dispersion determined by modeling was found to be (32.6 ± 0.5) mm/%(B·ρ).

2.2. Engineering

The final optics, magnetic, engineering design and manufacture of DGFRS-2 were carried out by the company SigmaPhi (France). The main characteristics of the DGFRS-2 quadrupole and dipole magnets are presented in Tables 2 and 3. The quadrupole lens Q1 focuses ERs in the vertical direction to match the D1-aperture. The quadrupoles Q2 and Q3 focus particles on the detector at the focal plane.

The D1 dipole magnet with a deflection angle of 31.5° and a gap between the poles of 132 mm (120 mm inside the vacuum chamber) focuses particles in the horizontal direction by the rotated rear pole face. The D2 dipole with a deflection angle of 10° and a gap of 120 mm (108 mm in the chamber) suppresses the background from scattered projectiles and high-energy protons or αs etc.

Table 2
Characteristics of the quadrupole magnets of DGFRS-2.

	Q-1	Q-2-3
Max. field gradient (T/m)	13.3	5.4
Max. current (A)	450	370
Bore diameter (mm)	150	300
Effective length (mm)	456	601
Max. power (kW)	28	62
Weight (t)	2.7	8.6

Table 3
Characteristics of the dipole magnets of DGFRS-2.

	D-1	D-2
Bending angle (deg)	31.5	10
Bending radius (m)	1.86	2.58
Max. current (A)	925	815
Max. field strength (T)	1.8	1.8
Pole gap (mm)	132	120
Max. power (kW)	140	97
Front pole face rotation	−8.4°	0.5°
Rear pole face rotation	−44.5°	0.3°
Weight (t)	28.0	6.8

3. Modeling of the "real" separator

After installing the separator on the beam line of the DC280 cyclotron, its main parameters were checked and refined. For the general testing of the ion-optical system α-particles emitted by the reference source ^{244}Cm were used. The use of both double-charged (99%) and single-charged (1%) αs (helium ions) made it possible to work with particles with magnetic rigidities differing exactly by a factor of 2.

For the modeling of trajectories of particles in the separator, tuning of its ion optical elements and calculation of the transmission, a code based on the GEANT4 framework was developed [24]. Magnetic field maps were computed using the OPERA-3D models based on the real geometry of magnetic elements. Trajectories of ^{252}No ions produced in the ^{48}Ca + ^{206}Pb(0.43 mg/cm^2) →^{252}No+2n reaction passing through DGFRS-2 simulated using GEANT4 platform are shown in Fig. 3.

The simulations, performed with the use of the actual dimensions and positions of the DGFRS-2 chambers and magnetic elements, resulted in values of its momentum dispersion of (33.1 ± 0.4) mm/%B·ρ. The ERs transmission for the ^{244}Pu(^{48}Ca,4n)^{288}Fl reaction at the target thickness of 0.4 mg/cm^2 was found to be 61%, that is very close to those obtained at the initial stage of the separator design (see Fig. 2).

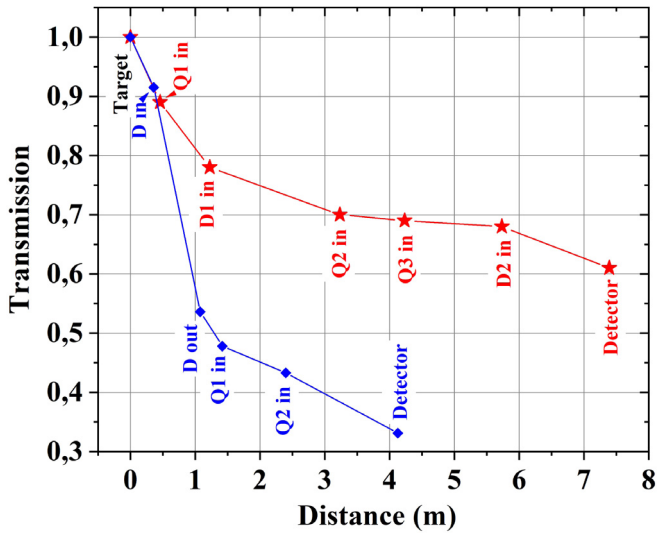

Fig. 4. Comparison of losses of ERs when passing through DGFRS-1 (at the ^{244}Pu target thickness of 0.3 mg/cm^2 blue lines with diamonds) and DGFRS-2 (red lines with stars).

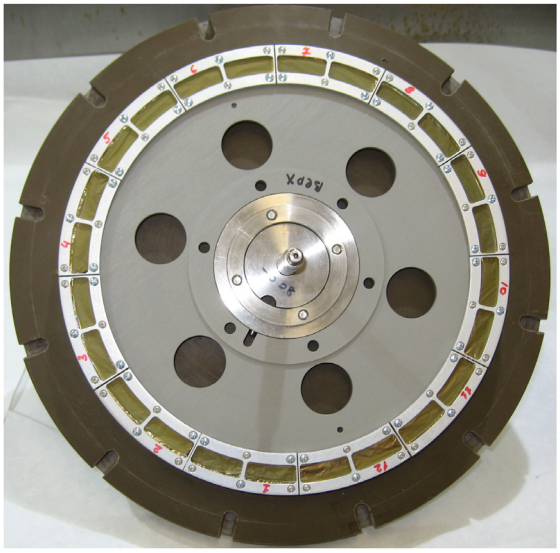

Fig. 5. The ^{242}Pu 24 cm rotating target wheel with 12 double sectors having 5.8 cm^2 area for each.

The developed modeling technique also made it possible to analyze the losses of ERs when passing through the separator. The results of this analysis are shown in Fig. 4.

As one can see from the figure the setting of a vertically focusing quadrupole in front of the dipole magnet and increasing its gap resulted in the improvement of transmission by the factor ≈2.

4. Systems of the DGFRS-2 separator

Next, we will describe the operation of the individual separator systems.

4.1. Target

Currently the method of electrolysis from organic solutions (molecular plating) is almost exclusively used for the manufacture of targets from isotopes of uranium and transuranic elements. This method allows one to produce homogeneous targets with a thickness of up to 1 mg/cm^2 with quantitative deposition yields above 95% [25–27].

Targets made of actinide isotopes for experiments on the synthesis of superheavy elements irradiated with ^{48}Ca, ^{50}Ti, ^{54}Cr etc. must withstand currents up to 10 pμA and integral beam doses above 10^{19} ions. The problem of creating such temperature-stable, long-lived targets has currently not been fully solved.

A partial solution to the problem is the application of a target in the form of a rotating disk (target wheel), where the segments with irradiated substance are located at the periphery. Due to the rotation the released power and the beam dose are distributed over a significantly larger area. Heating and cooling of stationary and rotating targets in vacuum and in gases have been studied, e.g. in [28–31]. It was found that the measured gain in the acceptable beam power can exceed a factor of 15–20 for a target rotating in helium compared to a stationary one in vacuum. According to calculations the hydrogen cooling should be even more effective.

A more detailed description of the processes that determine the durability of a target, including the heat exchange, radiation damage, sputtering and evaporation of backing and target material, is presented in [32].

The target system, developed for DGFRS-1, was used after several improvements in all experiments on the synthesis of SHE. The target wheel is rotated by an electric motor through a gear belt drive. This design allows the use of targets with a minimum diameter of the wheel of 10 cm (circumference ≈30 cm). The targets for the DGFRS-2 have a similar design (Fig. 5).

The possibility to accept higher beam current by increasing the rotation frequency and the diameter of the target is limited by mechanical loads, availability of target material and requirements for radiation safety. The maximum rotation frequency of the DGFRS-2 target wheel with the diameter of 24 cm can be up to 1000 rpm. To manufacture this target ≈70 mg of material are needed at a surface density of 1 mg/cm^2.

To monitor the status of the target, one performs a periodic measurement of the counting rate of α-particles emitted from it. The settings of magnetic elements are changed to transport α-particles, and the counting rate is measured by a focal detector for each segment without stopping the rotation. In test experiments, plutonium targets of 0.75 mg/cm^2 thickness were exposed to a ^{48}Ca beam with an intensity of up to 3 pμA with a total dose of up to 1.6×10^{19} ions without any noticeable loss of substance [33].

4.2. Handling of filling gas

To separate the gas-filled chambers of the separator from the high vacuum in the beam line, in experiments at DGFRS-1, a "rotating window" with 1.5 μm titanium foils was used. Long-term experiments with the beam intensity up to ≈1 pμA showed acceptable lifetime of the entrance window, ranging from several weeks to several months.

The situation changed dramatically during tests at DGFRS-2: at the beam intensity exceeding 2 pμA the entrance window was destroyed in just a couple of hours. Thus, the windowless differential pumping system was designed (see Fig. 1).

The required pressure is set due to dynamic equilibrium between gas bleed-in into the separator chamber through the controlled needle valve and pump-out. The pumping system of DGFRS-2 includes the roots pump, three turbomolecular pumps and a series of collimators and diaphragms. The system is automatically controlled, keeps the pressure constant inside the separator chamber with accuracy of ≈1% and is capable of reducing the gas pressure from about 1 mbar in the separator down to less than 10^{-7} mbar in the beam line.

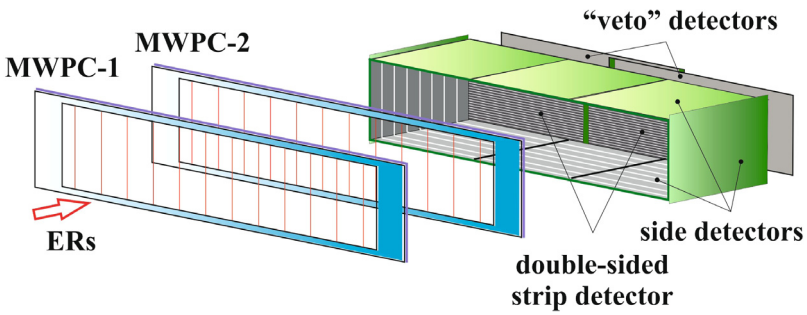

Fig. 6. Arrangement of the DGFRS-2 detection system.

4.3. Beam current monitoring

The traditional method of measuring the beam current using a Faraday cup cannot be used for gas-filled systems due to the ionization of the gas. At DGFRS-2, the beam is driven into water-cooled copper plate (stopper) designed to absorb up to 5 kW of beam power (20 pμA of ^{48}Ca at 250 MeV). The stopper chamber is electrically isolated from the chamber of the D1 magnet. The stopper plate is electrically connected to the chamber inside which it is installed (Fig. 1). The charge accumulated on the stopper chamber as a whole is measured by a digital integrator with an accuracy of 10%.

4.4. Detector system

The identification of synthesized nuclei is carried out after their implantation into position-sensitive detectors by the method of time, energy, and position correlations of ER with a chain of subsequent α-decays. The detector system of the separator DGFRS-2 is generally similar to that of DGFRS-1. It is composed of two multiwire proportional chambers (MWPC) and a position sensitive silicon detector array (Fig. 6). The detector module is separated from the hydrogen-filled volume by a 0.7 μm Mylar entrance window and it is filled with pentane at a pressure of 1.6 mbar. MWPCs are installed downstream the window at a distance of 65 mm from each other. The signals from MWPC make it possible to distinguish events caused by the arrival of a particle passing through the separator from the events of radioactive decays of nuclei implanted in the detector. The information about the flight time can also be recorded by the data acquisition.

A noticeably higher momentum dispersion of DGFRS-2 compared to DGFRS-1 required an increase of the detecting system which is limited by the size of the old detector chamber. In the first test experiments temporarily two double-sided silicon strip detectors BB-17 (DSSD, Micron Semiconductor, Ltd.) 300 μm thick were used as the focal plane stop detectors. Each DSSD has 1 mm wide strips, 48 horizontal on the front side and 128 vertical on the back side. Due to the overlapping of frames the second detector has only 84 strips open to the recoils, thus both detectors cover an area of 220 × 48 mm^2. Detectors of the same type located behind the stop detectors were used to generate a veto signal for charged particles with ranges greater than 0.3 mm.

The stop detectors are surrounded by eight 500 μm thick Si detectors (see Fig. 6) with the active area of 60 × 120 mm^2. They form the walls of the detector box serving to measure αs or fission fragments escaping from the stop detectors. Each side detector has eight 15-mm strips parallel to the surface of DSSDs. The new 240 × 60 mm^2 detectors, additional electronic modules and the new detector chamber are under preparation.

The position-averaged detection efficiency for full-energy α-particles is about 80%. Some α-particles can escape the focal detector in the backward hemisphere with deposited energy (E_{fd}) exceeding the registration threshold (E_{th}) and fly out of the detector box, or, conversely, they will be stopped in the side detector but with $E_{fd} < E_{th}$ (no signal in the focal detector). In such cases, the probability of including events in a chain of successive α-decays depends on the detector geometry, registration threshold, decay time, and background conditions when observing the chain.

The energy calibration of detectors was performed with α-particles emitted by implanted into the stop detector isotopes produced in nuclear reactions ^{170}Er(^{48}Ca,3-4n)^{214,215}Ra, ^{nat}Yb(^{48}Ca,xn)$^{215-217}$Th. The energies of fission fragments are determined by the same calibration coefficients. From comparison of the measured average energy of fission fragments of ^{252}No produced in the ^{206}Pb(^{48}Ca,2n) reaction and registered by both the focal-plane and side detectors with its known total kinetic energy, the sum energy loss of fission fragments was estimated to be about 20 MeV, see, e.g., [1,34].

4.5. Data acquisition system

On the new separator we use the data acquisition system, similar to that employed at DGFRS-1 [34,35]. The output signals from the charge sensitive preamplifiers (MESYTEC GmbH & Co) are split into analog and digital branches. The energy from all strips has been measured in one range 0.5 to 350 MeV. In order to handle with the available electronic modules, we reduced the number of vertical DSSD channels by combining two neighboring strips into one channel.

Along with ordinary signal processing the analog system generates under certain conditions, a signal that interrupts the accelerator beam. Such an interruption is desirable because the cyclotrons U400 and DC280 operate in the CW mode and in this case, the low-background mode of measurements — "beam off" should be organized by an external signal.

The analog system looks for sequences of events "implantation of ER — α-decay" correlating in position (1 DSSD pixel 1 × 2 mm^2) and time with predefined parameters [36]. The energy intervals for the implanted ER, subsequent α-particle(s) and time intervals in the sequence are set according to the reaction kinematics and the known or expected decay properties of the parent nucleus and its descendants.

The digital pulse processing is capable of extracting additional information from the signal shape analysis [37]. The digital analysis was in use at DGFRS-1 for the decay studies of superheavy nuclei [34,35]. The digital part of the data acquisition for DGFRS-2 was designed based on a system developed at Oak Ridge National Laboratory (ORNL) and the University of Tennessee Knoxville (UTK). This system is based on XIA Pixie-16 16-channel PXI Digital Pulse Processor modules (100 MHz, 14-bit sampling rate). Seventeen modules were assembled in two PXI creates to process signals from the silicon array, MWPCs, target and beam monitoring systems. Digitally controlled offsets were individually adjusted for each channel.

5. Results of test experiments

5.1. Position distribution of ERs on the focal plane

The horizontal and vertical distributions of reaction products on the focal plane determine the efficiency of their collection by the detector

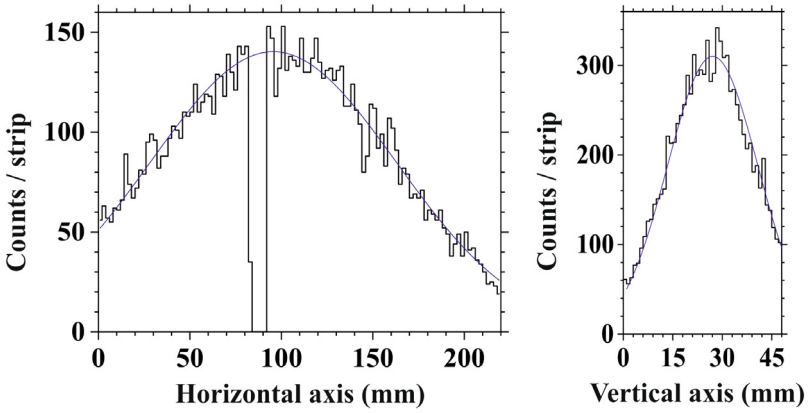

Fig. 7. Horizontal and vertical position distributions of ^{252}No on the focal plane, produced in the ^{206}Pb(^{48}Ca,2n) reaction. Lines show the Gaussian fits.

system. The widths of these distributions depend on the ion-optical characteristics of the set-up and the scattering of particles in the target, on the atoms of the filling gas, entrance window and pentane of the detector chamber. The horizontal and vertical position distributions of ^{252}No, produced in the reaction of 0.43 mg/cm^2 ^{206}Pb (in the form PbS) + ^{48}Ca (E_{lab} = 216 MeV) on the focal plane detector are presented in Fig. 7.

The shown distributions were recorded at the optimum gas pressure and magnet settings that correspond to the maximum collection efficiency of ERs by the detectors. The optimum magnet settings were estimated by calculations (see Section 3), which were then slightly varied to check the maximum yield. The dip in the horizontal distribution is caused by the frames between 2 parts of the stop detector.

5.2. Optimal gas pressure

The distribution of particles and efficiency of collecting recoils at the focal plane of the separator, along with the tuning of magnetic elements, are affected by processes related to the pressure of the working gas [4,6,38,39].

Initial charge equilibration. As is known, compound nuclei finalize their cooling by emitting of Auger-electrons. As a result one observes, for example for ^{192}Pb produced in the reaction ^{158}Gd(^{40}Ar,6n) [40] a charge distribution with $\bar{q} \approx 25$ and FWHM ≈ 20. The separator should be set to the equilibrated average charge. The required distance to reach the charge equilibrium at a low gas pressure can even exceed the distance to the first optical element.

Charge exchange. Calculations show that during the flight in the magnetic field between charge changing collisions an ion can travel far from the equilibrium trajectory. This effect broadens both the horizontal and vertical distributions of particles on the focal plane.

The effect of multiple scattering increases with increasing pressure. The formalism to describe this process can be taken e.g. from [41].

Despite the fact that the mentioned processes are qualitatively understandable, their quantitative description is very poor. Experimentally, the integral effect can be determined from the dependence of the widths of ERs distributions in the focal plane on the gas pressure.

The distributions of products of ^{170}Er(^{48}Ca,4n)^{214}Ra, ^{174}Yb(^{48}Ca,5n)^{217}Th, and ^{206}Pb(^{48}Ca,2n)^{252}No reactions in dependence on hydrogen pressure have been experimentally measured. The distributions were fitted by Gaussians and their standard deviations are presented in Fig. 8.

As expected, the width of the horizontal distribution decreases with increasing pressure, reaches a minimum at 0.9–2.0 mbar, and then monotonically increases (panel a). The width of the vertical distribution increases almost linearly with increasing pressure (panel b). The optimal gas pressure is in the vicinity of 0.9–1.3 mbar, where the maximum efficiency of particle detection by the focal plane detector is achieved (panel c).

5.3. Momentum dispersion of DGFRS-2

One of the most important characteristics of a separator is its momentum dispersion. The dispersion of a set-up is defined as $D = \Delta x/\Delta(B\cdot\rho)$, where Δx is the shift of the maximum of the distribution of particles transported through the device in the focal plane, $\Delta(B\cdot\rho)$ is the deviation in their magnetic rigidity. The momentum dispersions of known separators, including DGFRS-2, are compared in Table 1. High dispersion provides better resolution of reaction products and reduces the background. But realization of the high resolving power requires enlarged detectors and increases the sensitivity of the system to uncertainties in ionic charges and settings of magnets.

For the experimental determination of the momentum dispersion of DGFRS-2 shifts of maxima of distributions of ERs produced in the ^{170}Er(^{48}Ca,3-4n)^{214,215}Ra, ^{174}Yb(^{48}Ca,5n)^{217}Th, and ^{206}Pb(^{48}Ca,2n)^{252}No reactions in dependence on deviations of dipole settings were studied. The measured data in the range ±2% for the dipole D1 are presented in Fig. 9.

The experimentally determined momentum dispersion of (32.8 ± 0.3) mm/%($B\cdot\rho$) is in a good agreement with calculations presented in Sections 3 and 2.1.

5.4. Transmission

When interpreting the results and when planning experiments, information about the transmission of the set-up is necessary. This value can be determined by calculation, but to do this it is necessary to know the reaction cross-section and its dependence on the projectile energy. Other necessary parameters are: the thickness and composition of a target, as well as the energy of projectiles and beam dose on the target. The uncertainties in these values can lead to significant, up to the factor of 2, errors in the estimates of the transmission.

In measurements of the DGFRS-2 transmission, a target containing 0.43 mg/cm^2 of ^{206}Pb (in the form PbS) was bombarded by ^{48}Ca projectiles. Taking the reaction cross-section $\sigma_{2n} = (490^{+30}_{-20})$ nb from [42] we get a transmission of (59 ± 7)%, which exceeds that of DGFRS-1 by 30%–50% and is in agreement with the calculations discussed in Sections 3 and 2.1. Note that the estimated transmission would be larger if one applies the cross-sections measured more recently, e.g., $\sigma_{2n} = (426 \pm 2)$ nb [43], $\sigma_{2n} = (350 \pm 10)$ nb [44].

It was especially important to check the efficiency of the new separator in reactions leading to the synthesis of the superheavies. As a first check the reaction ^{243}Am(^{48}Ca,2-3n) leading to formation of moscovium isotopes was studied [45] and the results were compared with that of the experiments performed on DGFRS-1 [46]. Experimental conditions and results of studies are presented in Table 4.

As one can see, the new separator provides an efficiency more than twice as high as that of the DGFRS-1. The performed tests confirm

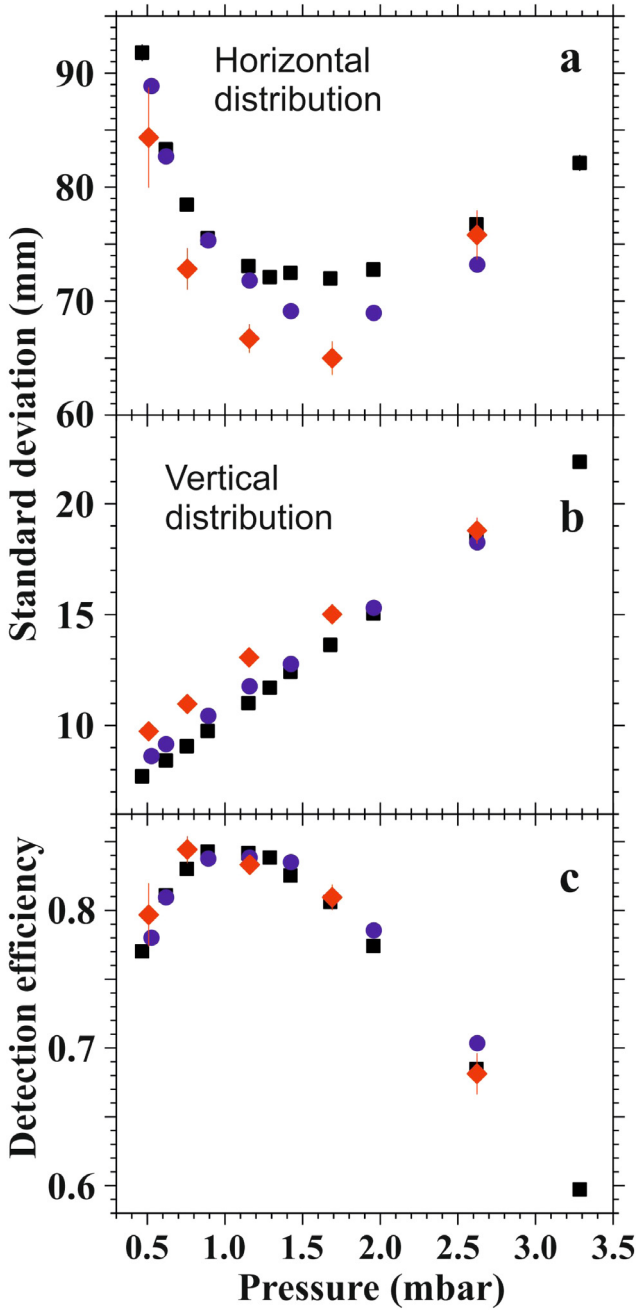

Fig. 8. Dependencies on hydrogen pressure of: horizontal (a) and vertical (b) distribution widths of ERs produced in ^{170}Er(^{48}Ca,4n)^{214}Ra (black squares), ^{174}Yb(^{48}Ca,5n)^{217}Th, (blue circles), and ^{206}Pb(^{48}Ca,2n)^{252}No (red diamonds) reactions, (c) collection probability of ERs by the detector with a size of 48 × 220 mm^2.

Table 4
Results of studies of the reactions ^{243}Am(^{48}Ca,2-3n) ^{288,289}Mc at DGFRS-1 and DGFRS-2.

	DGFRS-1	DGFRS-2
Target thickness (mg/cm^2)	0.37	0.36
^{48}Ca energy (MeV)	243.4	243.9
Beam dose 10^{18}	3.3	8.0
Decay chains of ^{288}Mc	6	30
Decay chains of ^{289}Mc	0	5
Gain factor	1	2.3 ± 0.2

the validity of the computer codes designed for the description of gas-filled separators (see Sections 3 and 2.1). This allows us to confidently calculate the settings of DGFRS-2 in future experiments on the synthesis of superheavy elements.

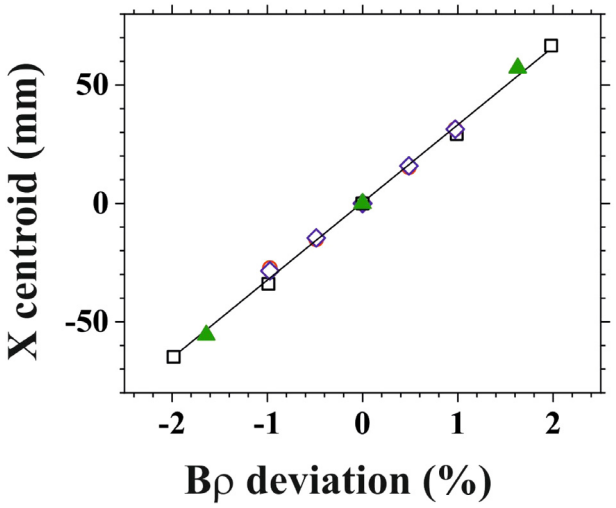

Fig. 9. Shifts of the horizontal distribution maxima of ERs produced in the ^{170}Er(^{48}Ca,3-4n)^{214,215}Ra (open blue diamonds and red circles, respectively), ^{174}Yb(^{48}Ca,5n)^{217}Th (open black squares), and ^{206}Pb(^{48}Ca,2n)^{252}No (solid green triangles) reactions in dependence on deviations of D1 dipole settings.

5.5. Background suppression

Along with the efficiency of collecting nuclei at detectors, an essential characteristic of the separator is its ability to suppress background particles — direct beam particles, scattered nuclei, and products of incomplete fusion reactions. Background suppression factors are particularly important when working with the DC280 cyclotron, since there the intensity of beams can be almost an order of magnitude higher than that provided by U400.

Fig. 10 shows the energy spectra of all particles registered in coincidence with MWPC signal (see Section 4.4) and of ^{252}No nuclei produced in the ^{206}Pb(^{48}Ca,2n) reaction using the separators DGFRS-1 and DGFRS-2. The shift in energy spectra originates mainly due to different energy losses of ERs in Mylar windows and pentane in the detector chamber.

From the comparison of the two panels, it is clear that when using DGFRS-2, the number of particles with energy above 9 MeV, that generated signals in MWPCs, practically coincides with the number of nobelium nuclei registered by the focal detector. This means that the new separator provides higher background suppression compared to the old one by the factor of about 200. This reduction of the background makes the search for decay events of implanted nuclei much more reliable and also prolongs the lifetime of the focal plane detectors.

6. Summary

The gas-filled separator DGFRS-2 is operating on-line to the DC280 cyclotron beam of the Super Heavy Element Factory of FLNR JINR. The magnetic system of the separator comprises the $Q_vD_hQ_hQ_vD$ scheme, the bending angle is (32 + 10)°, the distance from the target to the focal plane is 7.4 m, hydrogen is used as the working gas. The test results for collection efficiency of ERs from reactions with accelerated ^{48}Ca ions and background suppression showed that the new separator allows us to study the properties of superheavy elements formed in complete fusion reactions in the femtobarn cross-section range.

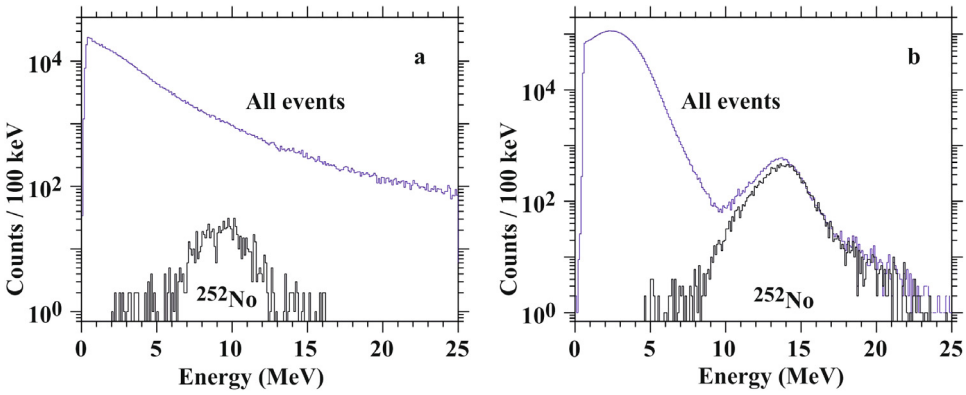

Fig. 10. Energy spectra of all particles registered by MWPC (upper blue line) and of the ^{252}No nuclei produced in the ^{206}Pb(^{48}Ca,2n) reactions (bottom black line), panel a — using separator DGFRS-1, b — DGFRS-2.

CRediT authorship contribution statement

Yu.Ts. Oganessian: Conceptualization, Methodology, Supervision. **V.K. Utyonkov:** Supervision, Data curation, Reviewing and editing. **A.G. Popeko:** Ion optical design, Writing, Reviewing and editing. **D.I. Solovyev:** Software, Validation, Investigation. **F.Sh. Abdullin:** Investigation. **S.N. Dmitriev:** conceptualization, Supervision. **D. Ibadullayev:** Investigation. **M.G. Itkis:** Conceptualization, Supervision. **N.D. Kovrizhnykh:** Software, Validation, Investigation. **D.A. Kuznetsov:** Engineering. **O.V. Petrushkin:** Engineering. **A.V. Podshibiakin:** Software. **A.N. Polyakov:** Software. **R.N. Sagaidak:** Investigation. **L. Schlattauer:** Software, Visualization. **I.V. Shirokovsky:** Investigation. **V.D. Shubin:** Investigation. **M.V. Shumeiko:** Software. **Yu.S. Tsyganov:** Software, Validation, Investigation. **A.A. Voinov:** Electroni design. **V.G. Subbotin:** Electronic design. **V.V. Bekhterev:** Engineering design. **N.A. Belykh:** Engineering. **O.A. Chernyshev:** Engineering. **K.B. Gikal:** Beam control systems. **G.N. Ivanov:** Engineering design. **A.V. Khalkin:** Radiation safety. **V.V. Konstantinov:** Engineering. **N.F. Osipov:** Engineering. **S.V. Paschenko:** Electronic design. **A.A. Protasov:** Beam control systems. **V.A. Semin:** Beam control systems. **V.V. Sorokoumov:** Electronic design. **K.P. Sychev:** Electronic design. **V.A. Verevochkin:** Engineering. **B.I. Yakovlev:** Engineering. **S. Antoine:** Engineering design. **W. Beeckman:** Engineering design. **P. Jehanno:** Engineering design. **M.I. Yavor:** Ion optical calculation. **A.P. Shcherbakov:** Ion optical calculation. **K.P. Rykaczewski:** Investigation, Reviewing and editing. **T.T. King:** Investigation. **J.B. Roberto:** Target design. **N.T. Brewer:** Investigation, Reviewing and editing. **R.K. Grzywacz:** Electronic design. **Z.G. Gan:** Software, Reviewing and editing. **Z.Y. Zhang:** investigation. **M.H. Huang:** Investigation. **H.B. Yang:** Investigation.

Declaration of competing interest

The authors declare the following financial interests/personal relationships which may be considered as potential competing interests: V.K. Utyonkov, A.G. Popeko, D.I. Solovyev, S.N. Dmitriev, M.G. Itkis, N.D. Kovrizhnykh, O.V. Petrushkin, A.N. Polyakov, M.V. Shumeiko, A.A. Voinov reports financial support was provided by Ministry of Science and Higher Education of the Russian Federation through the Grant No. 075-10-2020-117. K.P. Rykaczewski, T.T. King, J.B. Roberto, N.T. Brewer, R.K. Grzywacz reports financial support was provided by U.S. DOE Office of Nuclear Physics under DOE Contract No. DE-AC05-00OR22725 with UT Battelle, LLC. Z.G. Gan, Z.Y. Zhang, M.H. Huang, H.B. Yang reports financial support was provided by National Natural Science Foundation of China (Grant No. 11975279).

Acknowledgments

We thank the DC280 cyclotron crew and the associates of the ion-source group providing necessary beams of heavy ions and especially of stable high intensity ^{48}Ca. We are also grateful to team of the target laboratory of the chemistry of transactinides group for the skillful preparation of the targets.

These studies were supported by the Ministry of Science and Higher Education of the Russian Federation through the Grant No. 075-10-2020-117 and by the JINR Directorate grant.

Research at ORNL was supported by the U.S. DOE Office of Nuclear Physics under DOE Contract No. DE-AC05-00OR22725 with UT Battelle, LLC. This work was also supported by the National Natural Science Foundation of China (Grant No. 11975279).

References

[1] Yu. Ts. Oganessian, Heaviest nuclei from ^{48}Ca-induced reactions, J. Phys. G: Nucl. Part. Phys. 34 (4) (2007) R165–R242, http://dx.doi.org/10.1088/0954-3899/34/4/R01.

[2] Yu.Ts. Oganessian, V.K. Utyonkov, Superheavy nuclei from ^{48}Ca-induced reactions, Nuclear Phys. A 944 (2015) 62–98, http://dx.doi.org/10.1016/j.nuclphysa.2015.07.003.

[3] B.L. Cohen, C.B. Fulmer, Fission-fragment mass separator and the nuclear charge distribution of fission fragments of a single mass, Nucl. Phys. 6 (1958) 547–560, http://dx.doi.org/10.1016/0029-5582(58)90208-6.

[4] Yu.Ts. Oganessian, V.K. Utyonkov, Yu.V. Lobanov, F.Sh. Abdullin, A.N. Polyakov, I.V. Shirokovsky, Yu.S. Tsyganov, A.N. Mezentsev, S. Iliev, V.G. Subbotin, A.M. Sukhov, G.V. Buklanov, K. Subotic, Yu.A. Lazarev, K.J. Moody, J.F. Wild, N.J. Stoyer, M.A. Stoyer, R.W. Lougheed, C.A. Laue, Average charge states of heavy atoms in dilute hydrogen, Phys. Rev. C 64 (6) (2001) http://dx.doi.org/10.1103/PhysRevC.64.064309, 064309(1-6).

[5] K. Subotic, Yu. Ts. Oganessian, V.K. Utyonkov, Yu. V. Lobanov, F. Sh. Abdullin, A.N. Polyakov, Yu. S. Tsyganov, O.V. Ivanov, Evaporation residue collection efficiencies and position spectra of the Dubna gas-filled recoil separator, Nucl. Instrum. Methods Phys. Res. A 481 (1-3) (2002) 71–80, http://dx.doi.org/10.1016/S0168-9002(01)01367-5.

[6] K.E. Gregorich, Simulation of recoil trajectories in gas-filled magnetic separators, Nucl. Instrum. Methods Phys. Res. A 711 (2013) 47–59, http://dx.doi.org/10.1016/j.nima.2013.01.020.

[7] S. Dmitriev, M. Itkis, Yu. Oganessian, Status and perspectives of the Dubna superheavy element factory, EPJ Web Conf. 131 (08001) (2016) 1–6, http://dx.doi.org/10.1051/epjconf/201613108001.

[8] G.G. Gulbekian, S.N. Dmitriev, M.G. Itkis, Yu. Ts. Oganessyan, B.N. Gikal, I.V. Kalagin, V.A. Semin, S.L. Bogomolov, V.A. Buzmakov, I.A. Ivanenko, N.Yu. Kazarinov, N.F. Osipov, S.V. Pashenko, V.A. Sokolov, N.N. Pchelkin, S.V. Prokhorov, M.V. Khabarov, K.B. Gikal, Start-up of the DC-280 cyclotron, the basic facility of the factory of superheavy elements of the laboratory of nuclear reactions at the joint institute for nuclear research, Phys. Part. Nuclei Lett. 16 (6) (2019) 866–875, http://dx.doi.org/10.1134/S1547477119060177.

[9] Yu. Ts. Oganessian, Yu. V. Lobanov, A.G. Popeko, J. Rigol, F. Sh. Abdullin, V.V. Bekhterev, G.G. Gulbekian, A.A. Ledovskoy, V.N. Melnikov, S.P. Tretiakova, Yu. P. Kharitonov, Yu. S. Tsyganov, V.A. Chugreev, Gas-filled magnetic separator for nuclear reaction products on a heavy ion beam, in: Proceedings of the International Shool-Seminar on Heavy Ion Physics. Dubna, 3 – 12 October 1989, D7-90-142, JINR, 1990, pp. 44–51, (in russian).

[10] Yu. Ts. Oganessian, Yu. V. Lobanov, A.G. Popeko, F. Sh. Abdullin, G.G. Gulbekiayan, Yu. P. Kharitonov, A.A. Ledovskoy, S.P. Tretyakova, Yu. S. Tsyganov, V.E. Zhuchko, An attempt to synthesize element 110 in the reaction ^{40}ar+^{236}u and identify it using a gas-filled separator, in: Proceedings of the 6th Int. Conf. on Nuclei Far from Stability and 9th Int. Conf. on Atomic Masses and Fundamental Constants. Bernkastel-Kues, Germany, 1992. Inst. Phys. Conf, Vol. 132, 1992, pp. 429–432.

[11] V. Ninov, K.E. Gregorich, C.A. McGrath, The Berkeley gas-filled separator, AIP Conf. Proc. 455 (1) (1998) 704–707, http://dx.doi.org/10.1063/1.57362.

[12] D. Kaji, K. Morita, K. Morimoto, Y.L. Zhao, A. Yoneda, T. Suda, A. Yoshida, H. Kudo, K. Katori, I. Tanihata, Status of heavy element synthesis in RIKEN, J. Radioanal. Nucl. Chem. 255 (1) (2003) 77–80, http://dx.doi.org/10.1023/A:1022223613289.

[13] A. Semchenkov, W. Brüchle, E. Jäger, E. Schimpf, M. Schädel, C. Mühle, F. Klos, A. Türler, A. Yakushev, A. Belov, T. Belyakova, M. Kaparkova, V. Kukhtin, E. Lamzin, S. Sytchevsky, The TransActinide separator and chemistry apparatus (TASCA) at GSI – optimization of ion-optical structures and magnet designs, Nucl. Instrum. Methods Phys. Res. B 266(19–20) (2008) 4153–4161, http://dx.doi.org/10.1016/j.nimb.2008.05.132.

[14] D. Kaji, K. Morimoto, N. Sato, A. Yoneda, K. Morita, Gas-filled recoil ion separator GARIS-II, Nucl. Instrum. Methods Phys. Res. B 317(B) (2013) 311–314, http://dx.doi.org/10.1016/j.nimb.2013.05.085.

[15] A.G. Popeko, O.N. Malyshev, R.N. Sagaidak, A.V. Yeremin, Monte Carlo simulation of ion trajectories in the kinematic recoil separator vassilissa, Nucl. Instrum. Methods Phys. Res. B 126 (1-4) (1997) 294–296, http://dx.doi.org/10.1016/S0168-583X(96)01094-4.

[16] A.G. Popeko, On-line separators for the Dubna superheavy element factory, Nucl. Instrum. Methods Phys. Res. B 376 (1) (2016) 144–149, http://dx.doi.org/10.1016/j.nimb.2016.02.025.

[17] A. Yeremin, O. Malyshev, A. Popeko, A. Lopez-Martens, K. Hauschild, O. Dorvaux, Project of the experimental setup dedicated for gamma and electron spectroscopy of heavy nuclei at FLNR JINR, Nucl. Instrum. Methods Phys. Res. B 266 (19-20) (2008) 4137–4142, http://dx.doi.org/10.1016/j.nimb.2008.05.131.

[18] A.G. Popeko, O.N. Malyshev, A.V. Yeremin, S. Hofmann, Monte-Carlo optimization of the transmission of recoil separators, Nucl. Instrum. Methods Phys. Res. A 427(1–2) (1999) 166–169, http://dx.doi.org/10.1016/S0168-9002(98)01561-7.

[19] M. Yavor, Advances in Imaging and Electron Physics, Vol. 157, Elsevier, Amsterdam, Netherlands, 2009, http://dx.doi.org/10.1016/S1076-5670(09)01605-X,

[20] N. Bohr, Velocity-range relation for fission fragments, Phys. Rev. 59 (3) (1941) 270–275, http://dx.doi.org/10.1103/PhysRev.59.270.

[21] Y. Baudinet-Robinet, H.P. Garnir, P.D. Dumont, Statistical models for charge state distributions of heavy ions in carbon foils and gases, Phys. Lett. A 63 (1) (1977) 19–22, http://dx.doi.org/10.1016/0375-9601(77)90594-1.

[22] V.S. Nikolaev, I.S. Dmitriev, On the equilibrium charge distribution in heavy element ion beams, Phys. Lett. A 28 (4) (1968) 277–278, http://dx.doi.org/10.1016/0375-9601(68)90282-X.

[23] Yu. Ts. Oganessian, S.N. Dmitriev, Superheavy elements in D.I. Mendeleev's periodic table, Russ. Chem. Rev. 78 (12) (2009) 1077–1087, http://dx.doi.org/10.1070/rc2009v078n12abeh004096.

[24] D.I. Soloviev, et al., in press.

[25] Yu. V. Lobanov, G.V. Buklanov, F. Sh. Abdullin, A.N. Polyakov, I.V. Shirokovsky, Yu. S. Tsyganov, V.K. Utyonkov, Targets of uranium, plutonium, and curium for heavy-element research, Nucl. Instrum. Methods Phys. Res. B 397 (1) (1997) 26–29, http://dx.doi.org/10.1016/S0168-9002(97)00580-9.

[26] J. Runke, Ch. E. Düllmann, K. Eberhardt, P.A. Ellison, K.E. Gregorich, S. Hofmann, E. Jäger, B. Kindler, J.V. Kratz, J. Krier, B. Lommel, C. Mokry, H. Nitsche, J.B. Roberto, K.P. Rykaczewski, M. Schädel, P. Thörle-Pospiech, N. Trautmann, A. Yakushev, Preparation of actinide targets for the synthesis of the heaviest elements, J. Radioanal. Nucl. Chem. 299 (2) (2014) 1081–1084, http://dx.doi.org/10.1007/s10967-013-2616-6.

[27] S.N. Dmitriev, A.G. Popeko, High-power radioactive targets as one of the key problems in further development of the research program on synthesis of new superheavy elements, J. Radioanal. Nucl. Chem. 305 (3) (2015) 927–933, http://dx.doi.org/10.1007/s10967-014-3920-5.

[28] J.M. Nitschke, A high intensity heavy-ion recoil-target system, Nucl. Instrum. Methods 138 (3) (1976) 393–406, http://dx.doi.org/10.1016/0029-554X(76)90302-5.

[29] D. Marx, F. Nickel, G. Münzenberg, K. Güttner, H. Ewald, W. Faust, S. Hofmann, H.J. Schött, W. Thalheimer, A rotating target wheel with thintargets for heavy ion beams of high current densities, Nucl. Instrum. Methods 163 (1) (1979) 15–20, http://dx.doi.org/10.1016/0029-554X(79)90028-4.

[30] S. Antalic, P. Cagarda, D. Ackermann, H.-G. Burkhard, F.P. Heßberger, S. Hofmann, B. Kindler, J. Kojouharova, B. Lommel, R. Mann, S. Saro, H.-J. Schött, Target cooling for high-current experiments at SHIP, Nucl. Instrum. Methods Phys. Res. A 530 (3) (2004) 185–193, http://dx.doi.org/10.1016/j.nima.2004.04.217.

[31] N. Yu. Kazarinov, G.G. Gulbekyan, V.I. Kazacha, Stationary temperature distribution in a rotating ring-shaped target, Phys. Part. Nuclei Lett. 15 (3) (2018) 319–322, http://dx.doi.org/10.1134/S154747711803010X.

[32] R.N. Sagaidak, Durability of targets and foils irradiated by intense heavy ion beams in experiments on synthesis of superheavy nuclei, Phys. Part. Nuclei Lett. 14 (5) (2017) 747–761, http://dx.doi.org/10.1134/S1547477117050089.

[33] Yu. Ts. Oganessian, et al., in press.

[34] V.K. Utyonkov, N.T. Brewer, Yu. Ts. Oganessian, K.P. Rykaczewski, F. Sh. Abdullin, S.N. Dmitriev, R.K. Grzywacz, M.G. Itkis, K. Miernik, A.N. Polyakov, J.B. Roberto, I.V. Shirokovsky R.N. Sagaidak, M.V. Shumeiko, Yu. S. Tsyganov, V.G. Subbotin A.A. Voinov, A.M. Sukhov, A.V. Sabel'nikov, G.K. Vostokin, J.H. Hamilton, M.A. Stoyer, S.Y. Strauss, Experiments on the synthesis of superheavy nuclei ^{284}Fl and ^{285}Fl in the ^{239,240}Pu+ ^{48}Ca reactions, Phys. Rev. C 92 (034609) (2015) 1–10, http://dx.doi.org/10.1103/PhysRevC.92.034609.

[35] N.T. Brewer, V.K. Utyonkov, K.P. Rykaczewski, Yu. Ts. Oganessian, F. Sh. Abdullin, S.N. Dmitriev, J.G. Ezold, L.K. Felker, R.K. Grzywacz, M.G. Itkis, N.D. Kovrizhnykh, D.C. McInturff, K. Miernik, G.D. Owen, A.N. Polyakov, A.G. Popeko, J.B. Roberto, A.V. Sabel'nikov, R.N. Sagaidak, I.V. Shirokovsky, M.V. Shumeiko, N.J. Sims, E.H. Smith, V.G. Subbotin, A.M. Sukhov, A.V. Svirikhin, Yu. S. Tsyganov, S.M. VanCleve, A.A. Voinov, G.K. Vostokin, C.S. White, J.H. Hamilton, M.A. Stoyer, Search for the heaviest atomic nuclei among the products from reactions of mixed-Cf with a ^{48}Ca beam, Phys. Rev. C 98 (024317) (2018) 1–10, http://dx.doi.org/10.1103/PhysRevC.98.024317.

[36] Yu. S. Tsyganov, V.G. Subbotin, A.N. Polyakov, S.N. Iliev, A.M. Sukhov, A.A. Voinov, V.I. Tomin, Detection system for heavy element research: present status, Nucl. Instrum. Methods Phys. Res. A 525 (1-2) (2004) 213–216, http://dx.doi.org/10.1016/j.nima.2004.03.131.

[37] R. Grzywacz, C.J. Gross, A. Korgul, S.N. Liddick, C. Mazzocchi, R.D. Page, K. Rykaczewski, Rare isotope discoveries with digital electronics, Nucl. Instrum. Methods Phys. Res. B 261 (1-2) (2007) 1103–1106, http://dx.doi.org/10.1016/j.nimb.2007.04.234.

[38] A. Ghiorso, S. Yashita, M. Leino, L. Frank, J. Kallis, P. Armbruster, J. Dufour, P. Lemmeretz, SASSY, a gas-filled magnetic separator for the study of fusion reaction products, Nucl. Instrum. Methods Phys. Res. A 269 (1) (1988) 192–201, http://dx.doi.org/10.1016/0168-9002(88)90877-7.

[39] J. Khuyagbaatar, D. Ackermann, L.-L. Andersson, J. Ballof, W. Brüchle, Ch. E. Düllmann, J. Dvorak, K. Eberhardt, J. Even, A. Gorshkov, R. Graeger, F.-P. Heßberger, D. Hild, R. Hoischen, E. Jäger, B. Kindler, J.V. Kratz, S. Lahiri, B. Lommel, M. Maiti, E. Merchan, D. Rudolph, M. Schädel, H. Schaffner, B. Schausten, E. Schimpf, A. Semchenkov, A. Serov, A. Türler, A. Yakushev, Study of the average charge states of ^{188}Pb and ^{252,254}No ions at he gas-filled separator TASCA, Nucl. Instrum. Methods Phys. Res. A 689 (2012) 40–46, http://dx.doi.org/10.1016/j.nima.2012.06.007.

[40] N.K. Skobelev, V.Z. Maidikov, N.T. Surovitskaya, Some features of the ionization of nuclear reaction products, Z. Phys. A - Atoms Nuclei 314 (1) (1983) 5–7, http://dx.doi.org/10.1007/BF01411822.

[41] J.F. Ziegler, J.P. Biersack, U. Littmark, The Stopping and Range of Ions in Solids, Vol. 1, Pergamon, New York, 1985, http://dx.doi.org/10.1007/978-3-642-68779-2_5.

[42] Yu. Ts. Oganessian, V.K. Utyonkov, Yu. V. Lobanov, F. Sh. Abdullin, A.N. Polyakov, I.V. Shirokovsky, Yu. S. Tsyganov, A.N. Mezentsev, S. Iliev, V.G. Subbotin, A.M. Sukhov, K. Subotic, O.V. Ivanov, A.N. Voinov, V.I. Zagrebaev, K.J. Moody, J.F. Wild, M.A. Stoyer, R.W. Lougheed, Measurements of cross sections for the fusion-evaporation reactions ^{204,206,207,208}Pb+^{48}Ca and ^{207}Pb+^{34}s: Decay properties of the even-even nuclides ^{238}Cf and ^{250}No, Phys. Rev. C 64 (6) (2001) http://dx.doi.org/10.1103/PhysRevC.64.054606, 054606(1-8).

[43] B. Sulignano, S. Heinz, F.P. Heßberger, S. Hofmann1, D. Ackermann, S. Antalic, B. Kindler, I. Kojouharov, P. Kuusiniemi, B. Lommel, R. Mann, K. Nishio, A.G. Popeko, S. Saro, B. Streicher, M. Venhart, A.V. Yeremin, Identification of a K isomer in ^{252}No, Eur. Phys. J. A 33 (4) (2007) 327–331, http://dx.doi.org/10.1140/epja/i2007-10469-3.

[44] J.M. Gates, Ch. E. Düllmann, M. Schädel, A. Yakushev, A. Türler, K. Eberhardt, J.V. Kratz, D. Ackermann, L.L. Andersson, M. Block, W. Brüchle, J. Dvorak, H.G. Essel, P.A. Ellison, J. Even, U. Forsberg, J. Gellanki, A. Gorshkov, R. Graeger, K.E. Gregorich, W. Hartmann, R.D. Herzberg, F.P. Heßberger, D. Hild, A. Hübner, E. Jäger, J. Khuyagbaatar, B. Kindler, J. Krier, N. Kurz, S. Lahiri, D. Liebe, B. Lommel, M. Maiti, H. Nitsche, J.P. Omtvedt, E. Parr, D. Rudolph, J. Runke, H. Schaffner, B. Schausten, E. Schimpf, A. Semchenkov, J. Steiner, P. Thörle-Pospiech, J. Uusitalo, M. Wegrzecki, N. Wiehl, First superheavy element experiments at the GSI recoil separator TASCA: The production and decay of element 114 in the ^{244}Pu(^{48}Ca,3-4n) reaction, Phys. Rev. C 83 (5) (2011) http://dx.doi.org/10.1103/PhysRevC.83.054618, 054618(1-17).

[45] Yu. Ts. Oganessian, et al., in press.

[46] Yu. Ts. Oganessian, F. Sh. Abdullin, S.N. Dmitriev, J.M. Gostic, J.H. Hamilton, R.A. Henderson, M.G. Itkis, K.J. Moody, A.N. Polyakov, A.V. Ramayya, J.B. Roberto, K.P. Rykaczewski, R.N. Sagaidak, D.A. Shaughnessy, I.V. Shirokovsky, M.A. Stoyer, N.J. Stoyer, V.G. Subbotin, A.M. Sukhov, Yu. S. Tsyganov, V.K. Utyonkov, A.A. Voinov, G.K. Vostokin, Investigation of the ^{243}Am+^{48}Ca reaction products previously observed in the experiments on elements 113, 115, and 117, Phys. Rev. C 87 (1) (2013) http://dx.doi.org/10.1103/PhysRevC.87.014302, 014302.